



Contents lists available at ScienceDirect

Mechanical Systems and Signal Processing

journal homepage: www.elsevier.com/locate/ymssp

Narrowband feedback for narrowband control of resonant and non-resonant vibration



Sang-Myeong Kim*, Michael J. Brennan, Gustavo L.C.M. Abreu

Department of Mechanical Engineering, UNESP—Sao Paulo State University, Ilha Solteira 15385–000, SP, Brazil

ARTICLE INFO

Article history:

Received 15 May 2015

Received in revised form

26 January 2016

Accepted 30 January 2016

Available online 17 February 2016

Keywords:

Vibration control

Narrowband feedback

Narrowband control

Second order filters

Loudspeakers

ABSTRACT

This paper presents a simple feedback methodology that uses second order filters to control narrowband resonant and non-resonant vibration of a structural system. In particular, a single degree-of-freedom system is studied throughout the paper. The idea of the methodology is based on the fact that direct feedback is effective for in-phase vibration control. Thus, the position, velocity and acceleration are respectively fed back to control the low, resonant and high frequency vibration of the system. Each of these is passed through a band pass filter of second order that is inserted to extract and feed back the in-phase signal component only. This is called narrowband feedback. It is demonstrated with experiments that narrowband feedback is useful for narrowband control of resonant and non-resonant vibration.

© 2016 Elsevier Ltd. All rights reserved.

1. Introduction

Active control in the context of feedback control has generally meant *active damping control* that is aiming to reduce resonant responses of sound and vibration systems. This conception appears reasonable when the systems are all excited by an ideal broadband source (e.g., white noise and an impulse) and are further lightly damped. However, not all responses and systems ought to be controlled are resonant responses nor are necessarily lightly damped. For example, low frequency vibration is persistent in precision machines even if anti-vibration mounts are used [1]. The sound radiation to an acoustic free field is a phenomenon mostly in the high frequency region above the fundamental natural frequency of a moving-coil loudspeaker [2]. Vibration of a rotating or reciprocating machine is often dominated by harmonics of the operating frequency, which can occur at any frequencies including resonance and non-resonance frequencies [3]. Acoustic fields inside car cabins are indeed very highly damped [4]. Active control of such non-resonant sound and vibration in a highly damped system has been rarely reported in the literature. The paper presented here studies this, using a simple single degree-of-freedom (SDOF) vibration system.

There are many feedback methods that have been successful for resonant vibration control. Karnopp et al. [5] proposed direct velocity feedback in 1970s that feeds a velocity response back to the collocated force actuator through gain. They demonstrated with a SDOF system that the controller acts as an electrical damper. Balas [6] suggested that this could also be applied to multiple modal control of a flexible structure as long as the pair of sensor and actuator were truly collocated. Researchers soon realized that Balas's application tended to go unstable at high frequencies and thus instead proposed positive position feedback (PPF) in 1990s [7]. Unlike direct feedback (gain control), PPF is narrowband feedback that uses a low pass filter of second order as the controller so that it works effectively in the tuned frequency region while ineffectively at high frequencies. PPF is particularly suitable for

* Corresponding author. Fax: +55 18 3742 2992.

E-mail address: smkim123@hanmail.net (S.-M. Kim).

controlling the fundamental mode when a strain-type sensor is used. The electrical dynamic absorber (EDA) method was then proposed as a rather general tool for resonant vibration control, which is also narrowband feedback employing a number of second order filters [8–11]. Unlike PPF, however, it is a passivity-based controller (PBC) electrically realizing a mechanical dynamic absorber [9,10]. It is further a robust-PBC that is even more robust than Karnopp's electrical damper [8]. This method is also applicable to multiple modal control in both collocated and non-collocated control configurations, regardless of the types of transducers used [10,11]. Many other methods are also available in the control society, such as, classical compensators [12], state-based optimal methods [13], and intelligent methods like fuzzy control [14]. As such, active damping control for resonant vibration is a topic that has been extensively studied.

In this paper, a simple feedback methodology is presented for narrowband control of not only resonant but non-resonant vibration of a SDOF system. The idea is commonly based on the fact that direct feedback is effective for in-phase vibration control. Thus, the position, velocity and acceleration are respectively fed back to control the low, resonant and high frequency vibration of the system. Each of these is passed through a controller consisting of a band pass filter of second order. These are called narrowband position, velocity and acceleration feedback, respectively. It is well known that narrowband velocity feedback is a way of realizing an EDA for resonant vibration control [8]. The main focus of this paper is thus to investigate narrowband position and acceleration feedback for non-resonant vibration control. It is demonstrated with experiments that these two methods are respectively related to *active stiffness and inertia control*. They are thus useful for controlling the vibration at frequencies well below and well above the resonance frequency, respectively.

2. Theory of systems

Consider the active feedback control of a SDOF vibration system shown in Fig. 1(a), consisting of mass m_s , spring k_s and damper c_s . The SDOF system may represent a simple model of a resilient structure or a single vibration mode of a flexible structure. It is excited by the primary force $f(t)$ and controlled by the force $f_c(t)$ via the negative feedback controller $-C(j\omega)$, where t is time, ω is the angular frequency, and $j = \sqrt{-1}$. The systems before and after control can be represented by the two block diagrams shown in Fig. 1(b), where $P(j\omega)$ indicates the plant, $d(t)$ the disturbance signal, and $e(t)$ the error signal. The two signals $d(t)$ and $e(t)$ are physically the system responses (position, velocity or acceleration) measured by a common vibration sensor before and after control (i.e., disconnecting and connecting the feedback loop), respectively. Thus they cannot be measured simultaneously. Throughout this paper, the time dependence of signals is explicitly indicated (e.g., $e(t)$) while their frequency dependence is abbreviated (e.g., e) for simplicity.

2.1. Direct feedback

The dynamic equation of the SDOF system in Fig. 1(a) can be written as

$$m_s \ddot{w}(t) + c_s \dot{w}(t) + k_s w(t) = f(t) + f_c(t), \quad (1)$$

where $w(t)$, $\dot{w}(t)$ and $\ddot{w}(t)$ are the position, velocity and acceleration of the system in time, respectively. Let the control force be

$$f_c(t) = -[kw(t) + c\dot{w}(t) + m\ddot{w}(t)], \quad (2)$$

where k , c and m are non-negative and are the gains for direct position, velocity and acceleration feedback control, respectively. Combining Eqs. (1) and (2) gives the controlled system written as

$$[m_s + m]\ddot{w}(t) + [c_s + c]\dot{w}(t) + [k_s + k]w(t) = f(t). \quad (3)$$

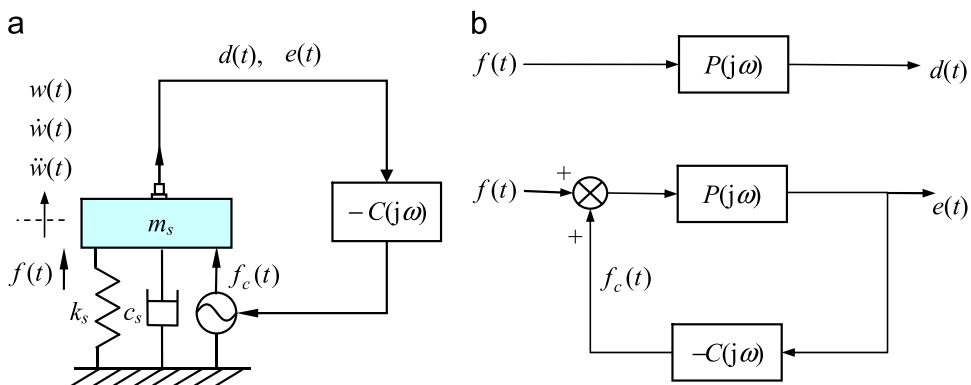


Fig. 1. Active vibration control of a SDOF system $P(j\omega)$ by the control force $f_c(t)$ with the negative feedback controller $-C(j\omega)$: (a) Schematic drawing and (b) the control block diagrams. The responses before and after control are $d(t)$ and $e(t)$, respectively.

It can be seen that the three control gains (m , c and k) act as an added mass, damper and spring, respectively. They may be called an electrical mass, damper and spring, respectively. It is thus clear that position feedback with k is effective at frequencies well below the resonance frequency (i.e., in the stiffness-controlled region) as it controls the stiffness [15]. Likewise, velocity feedback with c is effective at frequencies close to the resonance frequency (in the damping-controlled region); and acceleration feedback with m is effective at frequencies well above the resonance frequency (in the mass-controlled region). Note that each effective frequency region is also the region where each plant response is in-phase (0°) with the control force. This confirms the fact that direct feedback is effective for in-phase vibration control. Direct velocity feedback has been used for some specific applications such as active vibration isolation [1,5], where the plant responses tend to naturally and rapidly roll-off at high frequencies. In contrast, direct position and acceleration feedback have been rarely used because of some robustness problems that are addressed later in this paper.

2.2. Narrowband feedback

Rather than using direct feedback that may suffer from robustness problems, we consider narrowband feedback such that

$$f_c = - [kB_p(\omega)w + cB_v(\omega)\dot{w} + mB_a(\omega)\ddot{w}], \quad (4)$$

where w , \dot{w} , and \ddot{w} denote the position, velocity, and acceleration of the system in frequency, respectively. The variables are interrelated such that $\dot{w} = \dot{w}/j\omega$ and $w = \ddot{w}/(j\omega)^2$. The three terms inside the brackets in Eq. (4) correspond to narrowband position, velocity and acceleration feedback, respectively. Each filter is a band pass filter of second order given by

$$B_i(\omega) = \frac{j b_i \omega_i \omega}{\omega_i^2 - \omega^2 + j b_i \omega_i \omega}, \quad (5)$$

where $i = p, v$, and a ; ω_i the center frequency; and $b_i = 2\zeta_i$ the normalized bandwidth with the damping ratio ζ_i . This filter has been introduced to selectively extract and feed back the targeted in-phase signal component only. Thus, it should be tuned to a low frequency (in the stiffness-controlled region) for position feedback, the resonance frequency (in the damping-controlled region) for velocity feedback, and a high frequency (in the mass-controlled region) for acceleration feedback. These tuning rules may be respectively written as

$$\omega_p \ll \omega_s, \quad (6a)$$

$$\omega_v \approx \omega_s, \quad (6b)$$

$$\omega_s \ll \omega_a, \quad (6c)$$

where $\omega_s = \sqrt{k_s/m_s}$ is the angular natural frequency of the SDOF structural system. Combining Eqs. (1) and (4) gives the controlled system written as

$$[m_s + mB_a(\omega)]\ddot{w} + [c_s + cB_v(\omega)]\dot{w} + [k_s + kB_p(\omega)]w = f, \quad (7)$$

provided that it is stable. The three controllers, $mB_a(\omega)$, $cB_v(\omega)$ and $kB_p(\omega)$, act as an added mass, damper and spring within around the pass bandwidth of each filter, respectively. They may thus be called a narrowband electrical mass, damper and spring, respectively.

2.3. Passivity analysis

A single-input structural dynamic system such as that given by Eqs. (3) or (7) is said to be *passive* (i.e., unconditionally stable) if the driving point power is non-negative such that [16]

$$\text{Re}(\dot{w}^* f) \geq 0, \quad (\text{for all frequencies}) \quad (8)$$

where f and \dot{w} are respectively force and velocity at the driving point, and the superscript $*$ indicates the complex conjugate. It is trivial to assess the passivity of the system in Eq. (3) as it is a positive definite system by inspection such that $[m_s + m] > 0$, $[c_s + c] > 0$ and $[k_s + k] > 0$. The direct position, velocity and acceleration feedback controllers are thus PBCs, electrically realizing mechanical elements.

To assess the passivity of narrowband feedback, both sides of Eq. (7) are multiplied by \dot{w}^* and then the real parts are taken. It can be seen that only narrowband velocity feedback satisfies the passivity condition while the other two do not. The narrowband velocity feedback controller is thus a PBC, electrically realizing a narrowband damper (i.e., an EDA) as is well known [9]. Since the other two are not PBCs, however, the interpretations of the narrowband spring and mass are not exactly correct. They are though conceptually convenient and are also reasonable in an approximation sense within around the pass bandwidth of each filter. It can thus be finally stated that the narrowband position and acceleration feedback presented in this paper are methods to achieve narrowband stiffness and inertia control, respectively.

3. Theory of control

3.1. Basic theory

The analyses described in the previous section are valid if and only if the controlled systems are stable. The systems are further physically and lastingly realizable if and only if they are robust. A design technique for optimal, robust control [8,9] that has been particularly useful for vibration control is summarized in this subsection. The open loop frequency response function (FRF) $L(j\omega) = P(j\omega)C(j\omega)$ is explicitly described here as it is of paramount importance. For the SDOF system in Fig. 1 (a), the plants for position, velocity and acceleration feedback are respectively given by

$$P(j\omega) = (j\omega c_s)^{-1} \cdot A_s(\omega), \quad (9a)$$

$$P(j\omega) = c_s^{-1} \cdot A_s(\omega), \quad (9b)$$

$$P(j\omega) = (j\omega) c_s^{-1} \cdot A_s(\omega), \quad (9c)$$

where $A_s(\omega) = j2\zeta_s \omega_s \omega (\omega_s^2 - \omega^2 + j2\zeta_s \omega_s \omega)^{-1}$ in which ω_s the angular natural frequency and ζ_s the damping ratio. The corresponding controllers are respectively given by

$$C(j\omega) = k \cdot B_p(\omega), \quad (10a)$$

$$C(j\omega) = c \cdot B_v(\omega), \quad (10b)$$

$$C(j\omega) = m \cdot B_a(\omega), \quad (10c)$$

where again $B_i(\omega) = j2\zeta_i \omega_i \omega (\omega_i^2 - \omega^2 + j2\zeta_i \omega_i \omega)^{-1}$ in which $i = p, v,$ and a . Those for direct feedback can be obtained by setting $B_i(\omega) = 1$. Finally, Eqs. (9) and (10) are combined to form $L(j\omega)$.

With reference to the block diagram in Fig. 1(b), the control performance can be specified by the reduction ratio $S(j\omega) = e/d$ in which e and d are respectively the frequency domain representations of $e(t)$ and $d(t)$ that have been already defined in Section 2. This can be more conveniently written in decibel as

$$RR(\text{dB}) = 20 \log_{10} |S(j\omega)|, \quad (11)$$

where $S(j\omega) = [1 + L(j\omega)]^{-1}$ is also the sensitivity function. According to the Nyquist robustness criterion, the control system is then *stable* and *robust* with a degree of l_o if and only if its open loop FRF locus does not enclose or cross the circle of radius l_o centered at the instability point $(-1, 0)$. Thus, the robustness constraint for a stable controller can be written as

$$RR(\text{dB}) \leq 20 \log_{10} l_o^{-1}, \quad (\text{for all frequencies}) \quad (12)$$

where $0 < l_o < 1$ and the limiting value on the right hand side is the maximum allowable control spillover $RR_{\max} = 20 \log_{10} l_o^{-1}$. The task here is thus to find the controller in Eq. (10) that minimizes Eq. (11) within the control bandwidth of interest, subject to Eq. (12).

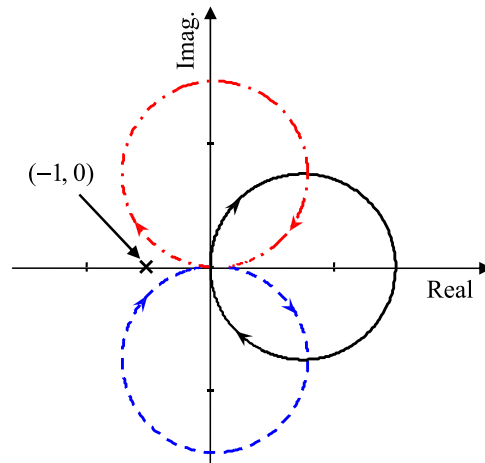


Fig. 2. Open loop FRFs for direct position (dashed line), velocity (solid), and acceleration (dash-dotted) feedback applied to the same SDOF plant of arbitrary coefficients. The arrows indicate the directions of increasing frequency.

3.2. Robustness analysis

According to the passivity analysis in Section 2.3, the three direct feedback controllers are all PBCs. They are thus in theory unconditionally stable such that, regardless of the control gains used, their open loop FRF loci will never cut through the negative real axis of the complex plane, i.e., $-180^\circ < \angle L(j\omega) < 180^\circ$ for all frequencies. However, not all of them are robust in physical realizations. This is illustrated in Fig. 2 that shows the individual open loop FRFs for the three methods [17]. It can be seen that direct velocity feedback is robust while the other two are not because their loci can be close to the instability point $(-1, 0)$ for a large gain. If these non-robust methods are attempted in practice, they are liable to go unstable. Typical causes to instability in a practical system are the time delay in the feedback loop, un-modeled dynamics, and uncertainties particularly at very low and very high frequencies [1,8].

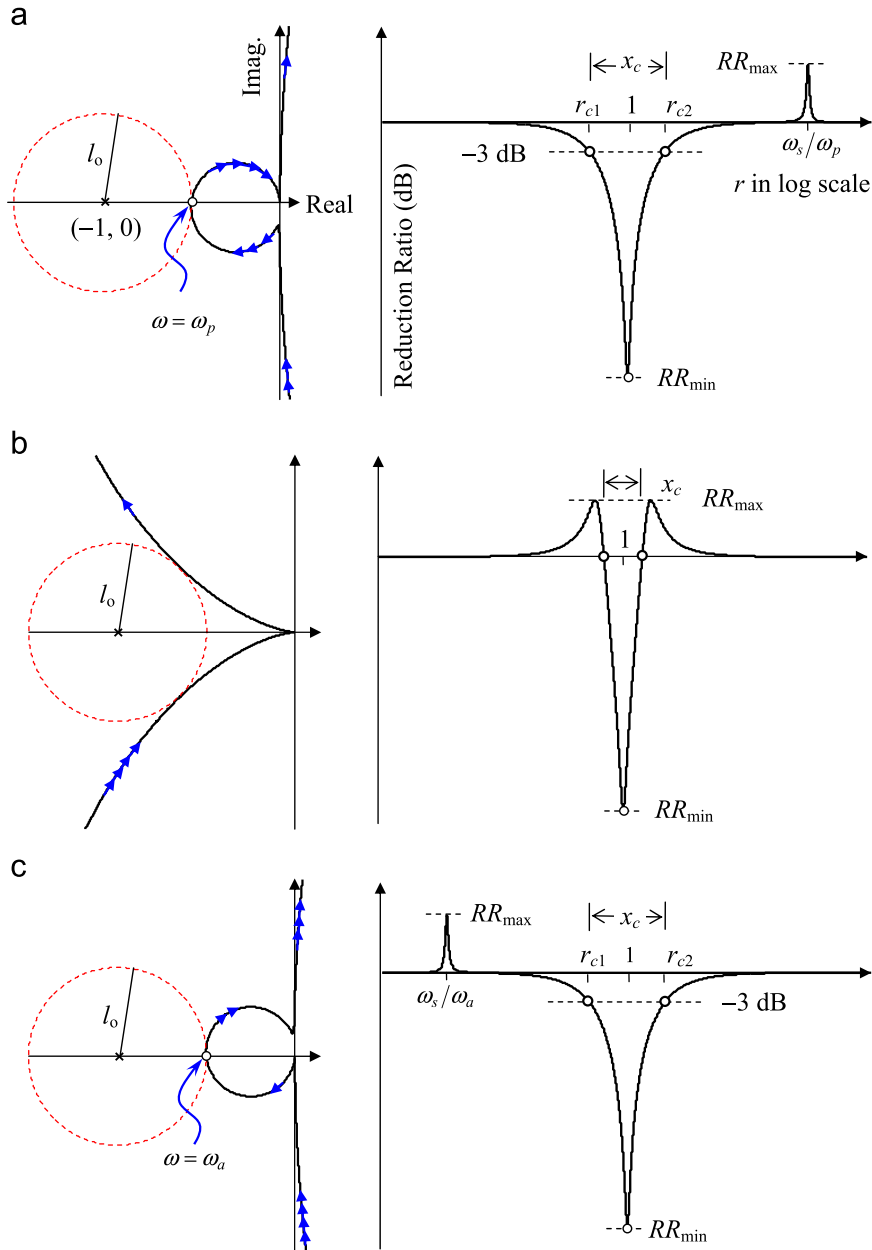


Fig. 3. Open loop FRF $L(j\omega)$ in Nyquist plot and the corresponding reduction ratio function $RR(\text{dB}) = 20\log_{10}|S(\omega)|$ against $r = \omega/\omega_j$ in logarithmic scale, applied to the same SDOF system: Narrowband (a) position, (b) velocity and (c) acceleration feedback control. The data used are $\zeta_s = 0.05$; $g = 20$; $l_0 = 1/2$; b is from Eq. (15) with $\eta = 30$ in (a) and (c) while this is from the Ref. [8] in (b). The arrows on each locus show the direction of increasing frequency starting from a single arrow. The reduction ratios are $RR_{min} = -20 \log_{10}(1+g)$ and $RR_{max} = 20 \log_{10}l_0^{-1}$.

The passivity analysis has also shown that the narrowband velocity controller is a PBC while the other two are not. It is interesting to examine if the other two can be nevertheless made to be “robust” (i.e., useful). To examine this, Fig. 3 illustrates the Nyquist plot of the open loop FRF and the corresponding reduction ratio function according to the control method: narrowband (a) position, (b) velocity and (c) acceleration feedback. Note that $r = \omega/\omega_i$ in the frequency axis so that $r = 1$ occurs at the tuned frequency: ω_p , ω_v and ω_a .

The Nyquist plots in Fig. 3 demonstrate that narrowband velocity feedback in (b) is unconditionally stable while the other two are not. The shape of the reduction ratio function in (b) is well known [8,9]; there is a notch at the target frequency with two spillover shoulders around it. The shapes are quite different in (a) and (c). It can be seen in (a) that the notch occurs at $\omega = \omega_p$ ahead of the peak at $\omega = \omega_s$. The trend is opposite in (c) where the peak occurs ahead of the notch. Fig. 3(a, c) illustrates that it is possible to have a deep notch (i.e., a large reduction) while limiting the height of the peak (i.e., a small spillover). From the analysis with Figs. 2 and 3, it can be stated that a PBC does not guarantee robustness. A PBC can be non-robust while a non-PBC can be robust.

It is also interesting to note that the two types of notches, in Fig. 3(a) and (c) and in Fig. 3(b), can be represented by conventional notch filters [18] as detailed in the Appendix. This implies that each reduction in Fig. 3 achieved by a feedback method can also be achieved by a feedforward method using a notch filter [19], and more importantly vice versa. Thus a narrowband feedback method presented in this paper may instead be applied whenever a feedforward method using a notch filter is inapplicable or ineffective in practice. In general, a feedback method performs more reliably against unmodeled dynamics and uncertainty, and is simpler in structure as no measurement is required on the primary sources.

3.3. Controller design

The design rules for narrowband velocity feedback have been presented elsewhere [8,9]. Those for narrowband position and acceleration feedback are described here using the plants given by Eqs. (9a) and (9c) and the controllers given by Eqs. (10a) and (10c). Since the minimum reduction ratio occurs at the target frequency ($\omega = \omega_i$) as illustrated in Fig. 3(a) and (c), applying Eq. (11) gives

$$RR_{\min} = -20 \log_{10}(1+g), \quad (13)$$

where the normalized controller gain is $g = k/k_s$ for position feedback or $g = m/m_s$ for acceleration feedback. Since the control bandwidth x_c is defined as the half-power bandwidth as illustrated in Fig. 3(a) and (c), applying $|S(jr)| = 1/\sqrt{2}$ gives [8]

$$x_c = gb \sqrt{1+2g^{-1}-g^{-2}}, \quad (14)$$

where the controller bandwidth is $b = b_p$ or $b = b_a$. This is also $x_c = r_{c2} - r_{c1}$ in which $r_{c1,c2} = (1/2)(\sqrt{x_c^2 + 4} \mp x_c)$. Since the maximum control spillover occurs at the plant natural frequency ($\omega = \omega_s$), applying Eq. (12) gives the constraint for (gb)

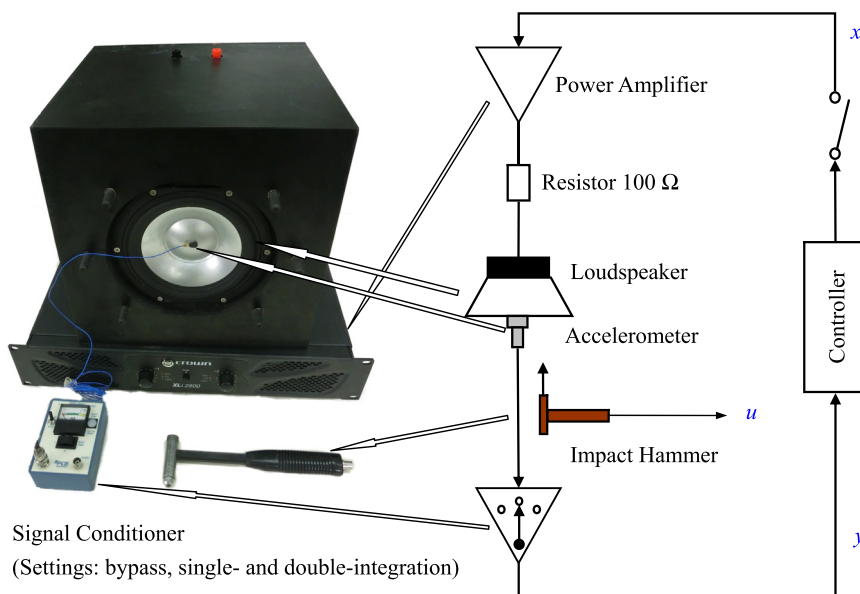


Fig. 4. Active vibration control of a moving-coil loudspeaker using an accelerometer.

written as

$$gb \leq 2\zeta_s \cdot \eta \cdot (1 - l_o), \tag{15}$$

where $\eta = \omega_s/\omega_p$ or $\eta = \omega_a/\omega_s$, and always $\eta > 1$ and $0 < l_o < 1$.

Therefore, the task here is to minimize Eq. (13) while maximizing Eq. (14), subject to Eq. (15). It can be seen that “the product of gain and bandwidth (gb)” of the control filter plays an important role: its amount is pre-determined by Eq. (15) and post-determines x_c in Eq. (14). Eqs. (14) and (15) indicate that, under a given degree of robustness l_o , the control bandwidth x_c related to (gb) can be improved if the structure is more highly damped (i.e., a greater ζ_s) and if the target frequency (ω_p or ω_a) is farther away from the plant natural frequency ω_s (i.e., a greater η). The former suggests that narrowband position and acceleration feedback are more effective in highly than lightly damped systems. The latter, which

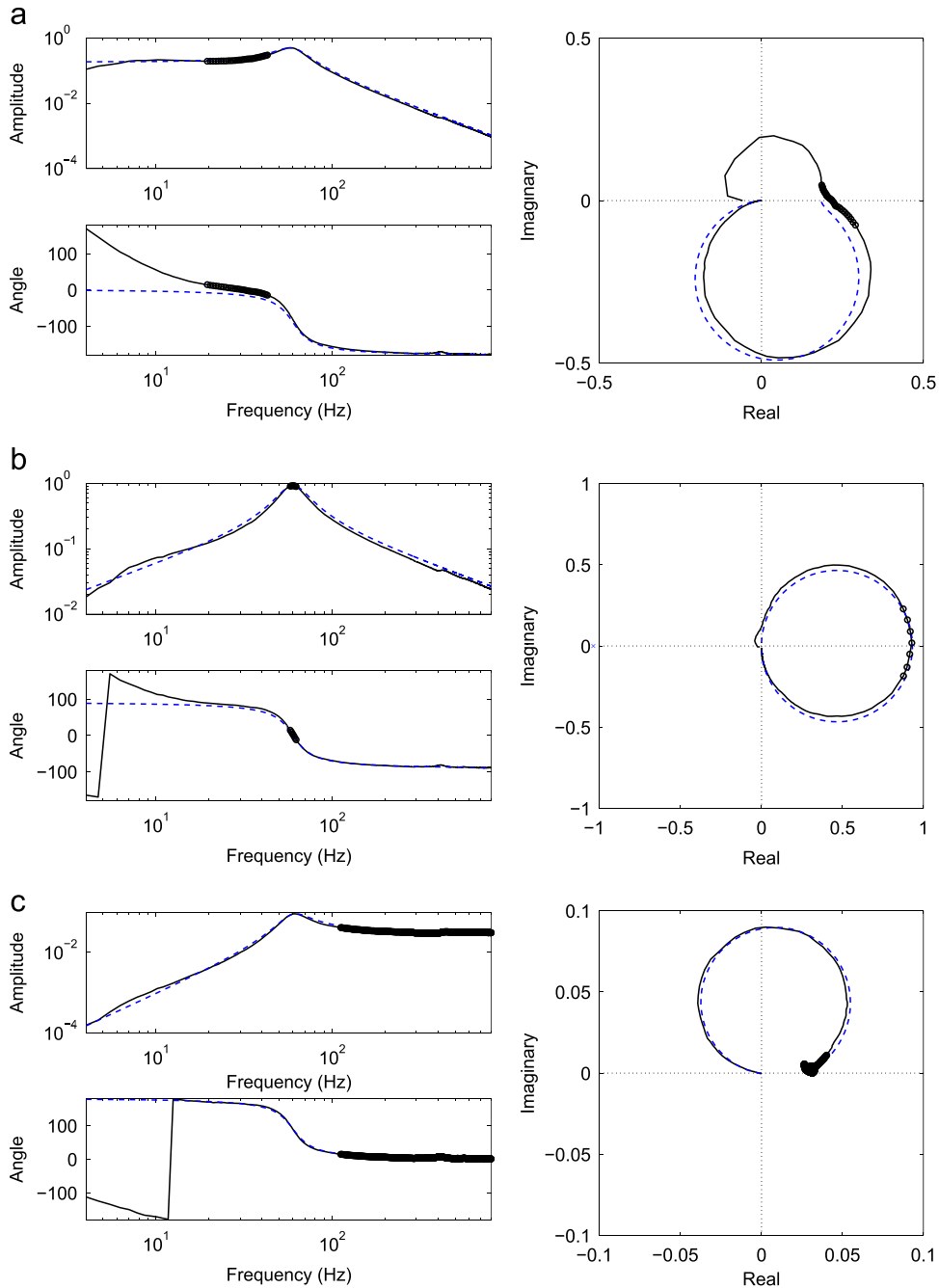


Fig. 5. Measured (solid lines) and identified (dashed) plant responses in Bode (amplitude: [V/V], phase: [degrees]) and Nyquist plots: (a) Position, (b) velocity, and (c) acceleration feedback.

suggests that they are also more effective at very low and very high frequencies, should though be practiced in caution since the model may become no longer reliable in these frequency regions because of un-modeled dynamics and uncertainty. Eqs. (13) and (14) then indicate that the amount of reduction can be improved without trading the control bandwidth, by way of increasing g and at the same time decreasing b to keep their product (gb) unchanged. It is thus in principle even possible to completely nullify the vibration at the target frequency.

4. Experiments

4.1. Experimental setup

A moving-coil loudspeaker was used to represent the SDOF system shown in Fig. 1. It is a Peerless HDS 6.5" loudspeaker with an aluminum cone, fixed into a cabinet with the exterior dimensions of 300 mm \times 300 mm \times 300 mm. It has a moving mass of 20 g, a suspension compliance of 804.8 $\mu\text{m}/\text{N}$, a mechanical Q factor of 3.3, an effective cone diameter of 13.1 cm, and DC resistance of 6.2 Ω . The experimental setup is shown in Fig. 4 together with a schematic diagram of the control loop. An accelerometer (PCB 352C22, 0.5 g) was attached to the center of the loudspeaker cone. It was then connected to a signal conditioner (PCB 480B10) with built-in integration circuits, enabling to selectively give the acceleration, velocity or position signal. A power amplifier (Crown[®] XLi 2500) was used to drive the loudspeaker via a resistor of 100 Ω (10 W) in series. The resistor was inserted so that the amplifier would behave as a current amplifier and consequently the loudspeaker system would behave more similar to an ideal SDOF system. Each of the narrowband feedback controllers in Eq. (10) was individually implemented in a DSP prototyping machine (dSPACE 1103) running at a sampling frequency of 32 kHz. The impulse invariant method was then used to obtain the discrete form for each controller [11]. Impact tests were finally conducted with a hammer (PCB 086C04) to measure the dynamic responses of the loudspeaker before and after control (i.e., disconnecting and connecting the loop) so as to assess the control performance.

The plant in Fig. 4 is the path between the input (denoted by x) to the power amplifier and the output (denoted by y) from the signal conditioner while the loop is disconnected. The signal conditioner was operated in three different settings: bypass, single- and double-integration to give the acceleration, velocity and position signal, respectively. Thus, there were

Table 1

Parameters of the plants and the narrowband feedback controllers.

Feedback	Parameters					
	Natural freq. $\omega_s/(2\pi)$	Damping ratio ζ_s	Gain k , c or m	Bandwidth b_i	Tuned freq. $\omega_i/(2\pi)$	Min. reduction ratio
Position	61	0.19	110	0.02	24 Hz	–25 dB
Velocity	61	0.19	12	1	61 Hz	–21 dB
Acceleration	61	0.19	600	0.02	150 Hz	–27 dB

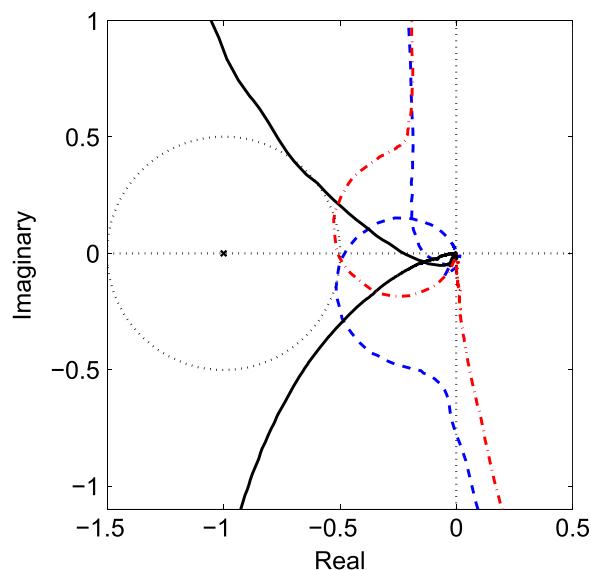


Fig. 6. Open loop FRFs for the narrowband position (dashed line), velocity (solid), and acceleration (dash-dotted) feedback. The circle (dotted) of radius $l_o = 0.5$ indicates the robustness boundary limit giving a maximum control spillover of 6 dB.

three different plants. The input and output signals were simultaneously monitored by a frequency analyzer (not shown) to produce the FRF of each plant. The measured (solid lines) FRFs of the three plants are shown in Fig. 5, where the Bode and Nyquist plots are shown for each plant. They were individually measured so that each FRF could contain any non-ideal artifacts of each operational setting within the practical signal conditioner. Also shown for comparison are the simulated FRFs (dashed) from the ideal SDOF models in Eq. (9). The natural frequency was 61 Hz and the damping ratio was 0.19, as

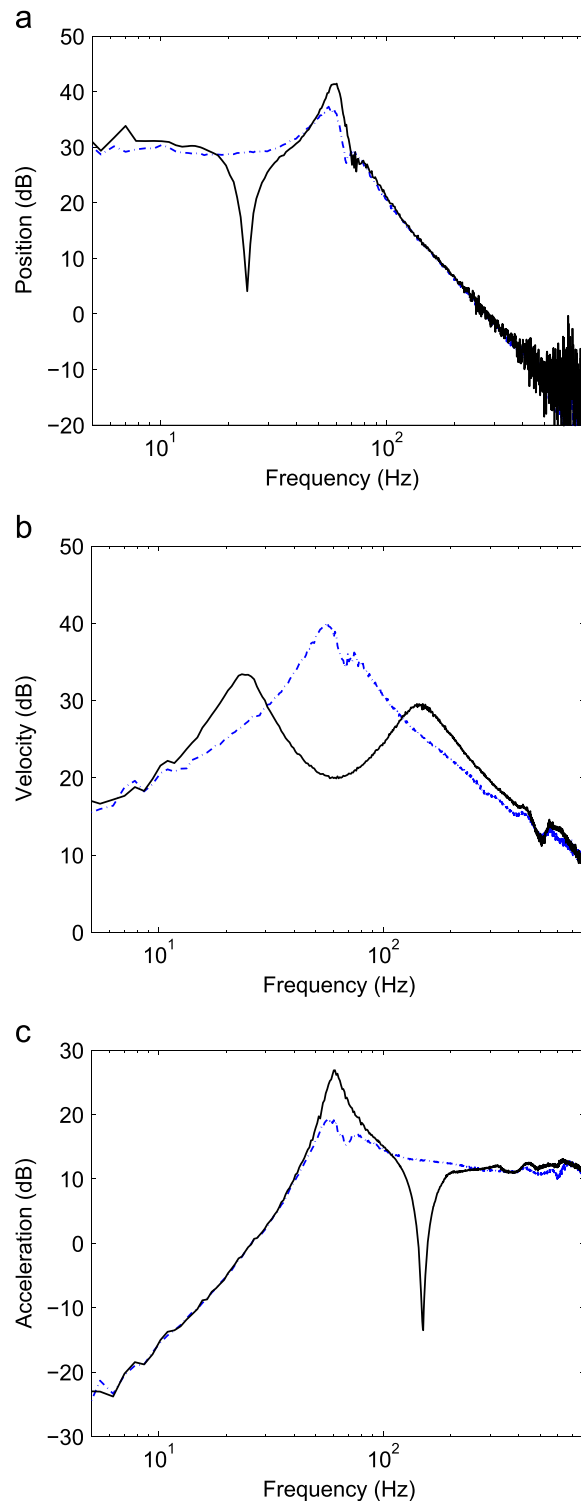


Fig. 7. Impact test results before (dash-dot lines) and after (solid) control for narrowband (a) position, (b) velocity, and (c) acceleration feedback.

given in Table 1. The symbols ‘o’ are additionally indicated in the range $|\angle G(j\omega)| \leq 15^\circ$ to emphasize the region around the in-phase frequency, where the degree of 15° was arbitrarily chosen. The measured and simulated responses agree well in general, except those at very low frequencies below about 20 Hz due largely to a high pass filter built-in to the power amplifier used.

4.2. Design and tests

In practice, it is often more convenient and accurate to design the controller based on measured data rather than a model such as that given by Eq. (9). A data-based graphical loop shaping technique was thus used to design each controller based on the measured plant response (solid lines) shown in Fig. 5. There are three parameters to determine of each control filter and the procedure is as follows: (i) choose the target frequency ω_i from those around the in-phase frequency according to Eq. (6), (ii) tune the gain (m , c or k) and the bandwidth b_i to maximize the performance in Eq. (11) subject to the robustness in Eq. (12). Either of the gain and the bandwidth can be chosen first and the other is then tuned. They then switch the order and redo the process. This is performed in a graphical way by repeatedly plotting the open loop FRF locus in the complex plane until a desirable shape is obtained. Knowledge of the model-based design rules given by Eqs. (13)–(15) can expedite the process. Fig. 6 shows the final desirable open loop FRFs designed for narrowband position, velocity and acceleration feedback control. It can be seen that each design allows a maximum control spillover of 6 dB (the dotted circle). The parameters of each control filter determined are also tabulated in Table 1.

The discrete form of each control filter was then implemented as shown in Fig. 4. Impact tests were finally conducted on the diaphragm of the loudspeaker before and after control. The hammer impact signal (denoted by u in Fig. 4) and the signal conditioner output signal (denoted by y) were simultaneously monitored by a frequency analyzer (not shown) to produce the FRF of each case. The impact test results obtained from the uncontrolled (dash-dot) and controlled (solid) systems are compared in Fig. 7. Note that each uncontrolled and the corresponding controlled response respectively correspond to the disturbance signal $d(t)$ and the error signal $e(t)$ in Fig. 1, with the hammer impact signal being $f(t)$. It is demonstrated in Fig. 7(a) and (c) that narrowband position and acceleration feedback are effective for controlling non-resonant vibration in the low and high frequency regions, respectively. The spillover at the natural frequency in each case is also evident. Fig. 7 (b) also demonstrates the effectiveness of narrowband velocity feedback for resonant vibration control. The maximum reductions achieved are tabulated in Table 1. It should be finally emphasized that the three effective narrowband control systems constructed are all robust with the maximum control spillover of 6 dB as can be seen in Figs. 6 and 7.

5. Conclusions

A narrowband feedback methodology has been presented for narrowband vibration control of a SDOF system. More specifically, narrowband position, velocity and acceleration feedback methods have been applied for narrowband stiffness, damping and inertia control in the low, resonant, and high frequency regions, respectively. Since narrowband damping control is well known, this paper has investigated the other two. It has been analytically shown that narrowband stiffness and inertia control are more effective in highly than lightly damped systems. It has been further shown that it is even possible in principle to completely nullify the vibration at the target frequency. Experimental work has also been presented to demonstrate that narrowband feedback is effective as well as robust for narrowband control of resonant and non-resonant vibration. Each control performance obtained is similar to that by a feedforward method using a notch filter, but is in fact by a feedback method using a second order filter.

Acknowledgments

We thank Professors J. A. Pereira, V. Lopes Jr. and Mr. C. J. Santana for their technical supports and comments.

Appendix A. Two notch filters

In relation to Fig. 3, the two notch filters of interest are

$$S_2(s) = [1 + g(\alpha\omega_s s)(s^2 + \alpha\omega_s s + \omega_s^2)^{-1}]^{-1}, \quad (A1)$$

$$S_4(s) = [1 + g\alpha\beta\omega_s\omega_v s^2(s^2 + \alpha\omega_s s + \omega_s^2)^{-1}(s^2 + \beta\omega_v s + \omega_v^2)^{-1}]^{-1}, \quad (A2)$$

where the coefficients are all positive, $s = j\omega$ is Laplace operator, and the subscripts 2 and 4 indicate the orders. $S_2(s)$ in bi-quadratic form represents the notches in Fig. 3(a) and (c) while $S_4(s)$ represents the notch with two shoulders in (b). It is important to note that these notch filters can be constructed by feedback methods [8]. In fact, $S_2(s)$ is the sensitivity function $S(s) = (1 + P(s)C(s))^{-1}$ of the feedback control system shown in Fig. 1 when a direct velocity feedback controller $C(s) = c$ is applied to a SDOF plant $P(s) = (1/c_s)\alpha\omega_s s(s^2 + \alpha\omega_s s + \omega_s^2)$ (the natural frequency ω_s , the gain $1/c_s$, and the bandwidth α) so

that $g = c/c_s$. Likewise, $S_4(s)$ is the sensitivity function when a narrowband velocity feedback controller $C(s) = c\beta\omega_v s(s^2 + \beta\omega_v s + \omega_v^2)$ (the center frequency ω_v , the gain c , and the bandwidth β) is applied to the same plant. Each of the notch filters can be characterized in terms of the center frequency, the depth and the stop bandwidth. They respectively correspond to the tuned frequency, the minimum reduction ratio and the control bandwidth in feedback control terms, as described in the main text of this paper.

References

- [1] S.M. Kim, S.J. Elliott, M.J. Brennan, Decentralized control for multichannel active vibration isolation, *IEEE Trans. Control Syst. Technol.* 9 (2001) 93–100.
- [2] M. Colloms, P. Darlington, *High Performance Loudspeakers*, sixth ed. John Wiley & Sons Ltd, Chichester, 2005, 27–44.
- [3] J.F. Wilby, Aircraft cabin noise and vibration prediction and passive control, in: M.J. Crocker (Ed.), *Handbook of Noise and Vibration Control*, Wiley, New York, 2007.
- [4] N. Lalor, H.H. Priebsch, The prediction of low- and mid-frequency internal road vehicle noise: a literature survey, *Proc. Inst. Mech. Eng. Part D: Automob. Eng.* 221 (2007) 245–269.
- [5] D. Karnopp, M.J. Crosby, R.A. Harwood, Vibration control using the semi-active force generators, *J. Eng. Ind.* 96 (1974) 619–626.
- [6] M.J. Balas, Direct velocity feedback control of large space structures, *J. Guid. Control* 2 (1979) 252–253.
- [7] J.L. Fanson, T.K. Caughey, Positive position feedback control for large space structures, *AIAA J.* 28 (1990) 717–724.
- [8] S.M. Kim, S. Pietrzko, M.J. Brennan, Active vibration isolation using an electrical damper or an electrical dynamic absorber, *IEEE Trans. Control Syst. Technol.* 16 (2008) 245–254.
- [9] S.M. Kim, S. Wang, M.J. Brennan, Dynamic analysis and optimal design of a passive and an active piezo-electrical dynamic vibration absorber, *J. Sound Vib.* 330 (2011) 603–614.
- [10] S.M. Kim, S. Wang, M.J. Brennan, Comparison of negative and positive position feedback control of a flexible structure, *Smart Mater. Struct.* 015011 (2011) 10.
- [11] S.M. Kim, J.E. Oh, A modal filter approach to non-collocated vibration control of structures, *J. Sound Vib.* 332 (2013) 2207–2221.
- [12] A. Preumont, *Vibration Control of Active Structures: An Introduction*, Kluwer Academic Publishers, Dordrecht, 1997.
- [13] F.L. Lewis, V.L. Syrmos, *Optimal Control*, second ed. John Wiley & Sons, Inc, New York, 1995.
- [14] G.L.C.M. Abreu, J.F. Riberiro, A self-organizing fuzzy logic controller for the active control of flexible structures using piezoelectric actuators, *Appl. Soft Comput.* 1 (2002) 271–283.
- [15] R.J. Peters, B.J. Smith, M. Hollins, *Acoustics and Noise Control*, third ed. Taylor & Francis, New York, 2011.
- [16] P. Triverio, S. Grivet-Talocia, M.S. Nakhla, F.G. Canavero, R. Achar, Stability, causality, and passivity in electrical interconnect models, *IEEE Trans. Control Syst. Technol.* 30 (2007) 795–808.
- [17] M.J. Brennan, K.A. Ananthganesan, S.J. Elliott, Instabilities due to instrumentation phase-lead and phase-lag in the feedback control of a simple vibrating system, *J. Sound Vib.* 304 (2007) 466–478.
- [18] D. Self, *The Design of Active Crossovers*, Elsevier, Inc, London, 2011.
- [19] Z. Mohamed, J.M. Martins, M.O. Tokhi, J. Sá da Costa, M.A. Botto, Vibration control of a very flexible manipulator system, *Control Eng. Pract.* 13 (2005) 267–277.